

## Feasibility of 5-axis CNC friction stir welding of Aluminum 3003-H14

Austin CLARK<sup>1,2,a</sup>, Ihab RAGAI<sup>2,b\*</sup>, Gianluca BUFFA<sup>3,c</sup> and Livan FRATINI<sup>3,d</sup>

<sup>1</sup>GROB Systems Inc., Bluffton, OH 45817, USA

<sup>2</sup>The Pennsylvania State University, Erie, PA 16563, USA

<sup>3</sup>Department of Engineering, University of Palermo, Viale Delle Scienze, 90128 Palermo, Italy

<sup>a</sup>aclark@grobssystems.com, <sup>b</sup>ihab.ragai@psu.edu, <sup>c</sup>gianluca.buffa@unipa.it,

<sup>d</sup>livan.fratini@unipa.it

**Keywords:** FSW, 5-Axis CNC, Aluminum 3003, Process Parameters

**Abstract.** This article investigates the effects various Friction Stir Welding (FSW) parameters have on the Ultimate Tensile Strength (UTS) of AA3003-H14 joints welded in a horizontal 5-axis CNC. The goal of this research is to combine the use of horizontal 5-axis machining with the ability to FSW in parallel. Two different tools were used in these tests. Both tools had tapered cylindrical pin profiles, while shoulder diameters were 19 mm and 25.4 mm, respectively. Along with the aforementioned tool shoulders, various tool rotation speeds and feed rates were evaluated with tensile tests conducted across 11 variable sets. A constant axial force of 5.2 kN was maintained during welding. A 25.4 mm tool shoulder was found to yield higher UTS than a 19 mm shoulder with the same feed rate and tool rotation speed. While feed rate had some effect on the strength of the weld, tool rotation speed did not have a significant effect on the tensile results in this study. The parameter set with the highest tensile strength in this test was performed with a 25.4 mm tool shoulder, tool rotation speed of 1200 rpm and a feed rate of 100 mm/min.

### Introduction

FSW is a solid-state welding process which allows materials to be joined below their melting point by use of pressure and frictional heat generated by rotation of a tool [1]. Since its introduction in 1991, FSW has gained popularity in industries such as automotive, aerospace, and electronics [2]. A benefit of FSW is the ability to join dissimilar materials as a solid-state bond is created without requiring the base material to reach a melting temperature. A key advantage of FSW over arc welding is the reduced thermal input at the heat affected zone (HAZ). Since the base material does not reach melting temperature in FSW, mixing occurs from plastic deformation in the weld seam at lower temperatures as compared to traditional arc welding. Advantages to welding below the liquid phase are a reduced risk of porosity, solidification cracking, and solute redistribution as noted by Singh [3]. FSW was found to have a 27% lower heat input than TIG and a 51.2% lower heat input than MIG welding on Aluminum test samples [4]. The reduced heat input of FSW as compared to arc welding was also found to have superior fatigue strength when compared to TIG welding as noted by Takhakh. The endurance limit of FSW AA3003 was 52 MPa while TIG welds yielded 41 MPa [5]. Mypati reported that using FSW to bond micro-sheets of copper and aluminum together for use in EV battery packs can result in an increase in corrosion resistance due to the formation of intermetallic compounds formed from the heat generated during welding [6].

AA3003 Applications and Use: Aluminum 3003 is widely used in construction for its formability, weldability and corrosion resistant properties. It is often used in heat exchangers where high thermal conductivity and formability properties are beneficial for use in parts such as fins in heat exchangers. Thin-walled fins are commonly extruded or rolled and then brazed together. Mechanical properties of the extruded or rolled aluminum, which includes work hardening from the forming process, are generally degraded after the brazing process heats the

material to a high enough temperature to cause grain elongation [7]. To maintain mechanical properties of this alloy in joining operations, FSW can be used to reduce heat input and maintain properties such as hardness and ultimate tensile strength (UTS). In a study on mechanical effects on FSW AA3003, Della et al. noted that fine grain recrystallization occurring in the stir zone (SZ) increased hardness above the HAZ while peak hardness in the SZ was 88% that of the base metal (BM) [8].

FSW in 5-Axis CNC: When machining surfaces that are to be welded, the surface finish along the weld seam plays a crucial part in final weld integrity. Due to the inherent characteristics of aluminum being a highly ductile material, long chips are produced during machining. These long chips can collect on the surface and reduce surface quality if not cleared regularly [9]. In a 3-axis vertical mill, the chips must be manually removed from the surface. Utilizing a horizontal 5-axis CNC, where falling chips minimally contact the workpiece can improve characteristics of surface finish, but also reduces tool wear and machining force as well [10]. Forces such as traverse, side, axial and torque are enacted on the X, Y, Z, and spindle axes respectively [11]. The addition of two rotational axes allows greater flexibility in machining complex part geometries and can reduce overall process time by performing more machining in a single operation. Interestingly, İzol reported an increase in machining time on an identical part with a 5-axis machine compared to a 3-axis due to the additional motion in tool optimization in the 5-axis CNC [12]. However, Bolaga et al. noted that any extended machining time for part complexity is mitigated by reducing additional cutting operations and set up time in a 3-axis CNC as compared to performing all of the machining in a 5-axis machine [13]. Another benefit of 5-axis capabilities over 3-axis in FSW is the ability to introduce tooling tilt. This tilting of the tool, in the direction of welding, also known as traverse direction, has been found to improve distribution of heat input along the welded joint [14]. This reduction in heat has been found to reduce weld flash along the trailing edge of the weld [15]. This improved heat distribution can also improve the quality of the weld by suppressing voids due to more equiaxed mixing of the material [16]. This tooling tilt during welding, in combination with a tool such as an A-Skew™ probe, improved mixing and increased weld nugget size in butt and lap joints when tested on 6 mm Aluminum plate by TWI [17]. When noting the importance of utilizing a tooling tilt, Goyal found that the effects on UTS in FSW AA3003 were nearly identical between feed rate and tooling tilt angle [18]. When utilizing the capabilities of a 5-axis CNC, the ability to FSW curved surfaces becomes possible. Industrial applications involving machining highly precise, complex geometrical parts with curved surfaces, often require multiple parts joined together such as with fluid impellers, turbine blades and heat exchanger fins as mentioned previously. In most 5-axis machining applications, these highly complex parts must be removed from the CNC before being joined and eventually returned to the CNC for final processing and dimensioning. Combining 5-axis machining and FSW mitigates multiple handling of parts requiring these processes. Although, FSW of curved surfaces is much more difficult than planar surfaces due to the additional motion and on-the-fly interpolation in the direction that welding force is being applied. A Finite Element Analysis (FEA) for FSW curved surfaces was conducted by Meyghani et al. which used a mesh surface that could account for mechanical deformation due to thermal input from the tool [19]. In this simulation, tooling tilt had to be used to maintain constant contact with the curved surface. In an experiment using a robot and constant force control when FSW curved surfaces, Xiao et al. discovered that depending on positive or negative curvature, actual compressive axial forces are less than or greater than device input forces respectively [20]. It has also been found that the ability to monitor motor torque to adjust position and control force improves weld quality as opposed to welding with a fixed position in the Z-axis. Torque control was also found to maintain weld power stability better than force control as torque and tool rotation speed directly affect weld power [21]. This was found to reduce potential defects by improving material flow within the weld zone in AA6061 [22].

Further effects on weld strength, represented by the ultimate tensile strength (UTS) in FSW of AA3003, found that increasing the feed rate above 1500 mm/min reduced the joint's UTS [23]. A counter to this is a loss in welding efficiency with lower feed rates, which may result in higher UTS, but increase thermal input into the tool and base material. It should be noted that there is a limit to the reduction in feed rate that reaches a point where excessive heat will soften the weld nugget and reduce UTS. This was observed by Takhakh in a study where travels speeds below 80 mm/min adversely affected the UTS of AA3003 [24]. This point is further reinforced by a study where feed rates below 80 mm/min and tool rotation speed below 1000 rpm exhibited tunnel-type defects at 500 rpm [25].

### Testing Methodology

The FSW work conducted herein utilized a GROB G552T Universal Milling-Turning Machining Center. A butt joint was welded using two 6.35 mm plates of AA3003. Table 1 lists the nominal chemical and mechanical properties of AA3003. All plates were fastened to a machine pallet in the position of welding with all welds being 40 mm in length as shown in Fig. 1. The FSW tool used for testing was made from A2 steel. The FSW tool used in this study had a cylindrical taper profile for the pin with no tooling tilt used. In studies conducted by Shalin and Hiten, a cylindrical tapered pin profile resulted in higher UTS than pins with cylindrical or square profiles [26].

*Table 1 – Aluminum 3003-H14 chemical & mechanical properties [27].*

Chemical Composition					
Mn	Fe	Si	Cu	Zn	Others
1.00 - 1.50	0.70	0.60	0.05 - 0.20	0.10	0.15
Physical & Mechanical Properties					
Density (kg/m <sup>3</sup> )	Elastic Modulus (GPa)	Hardness (Brinell)	Thermal Conductivity (W/m.K)	Tensile Strength (MPa)	Yield (MPa)
2730	69	40	159	150	85

The pin length of 4 mm is 63% the base material thickness. The FSW tool was designed for maximum surface area contact at the mating surface of the tool holder, while tapering down to the specified shoulder diameter for welding, as shown in Fig. 2. In future tests, cut and etch may be utilized to measure actual weld size. An HSK-100A tool holder was used in conjunction with a spindle capable of a tool rotation speed of 14,500 rpm and 261 N·m of torque [28]. To achieve and maintain the required force during welding, a custom software cycle for adaptive force monitoring and control was used in testing. Initially, the Z-Axis motor torque, which was adjusted in increments of 5 N·m, was used to convert a pre-defined motor torque setting to axial force at the tool. A 5 N·m of motor torque resulted in a 1.04 kN axial force. An initial range of 4.16 – 6.24 kN was tested with an axial force of 5.2 kN yielding the best surface finish without voids or excessive surface flash and indentation. Therefore, for the experiments reported herein, the axial force was programmed to maintain 5.2 kN during the entire weld path, which was held within 3% of programmed force for all welds.

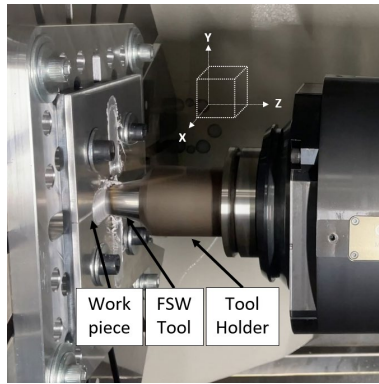


Figure 1 – Test Setup.

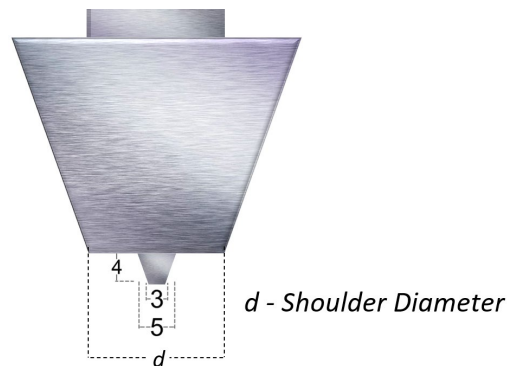


Figure 2 – FSW tool geometry (dim. in mm).

For the current study, the experimental parameters included tool shoulder diameter, tool rotation speed and feed rate. In other works, a tool shoulder diameter 3x the material thickness was shown to have the most beneficial effect on the grain structure in FSW of Magnesium alloys [29]. Also, in AA6061, UTS with shoulder diameters three times material thickness was found to be higher than tools with shoulder diameters of 2.5x and 3.5x material thickness [30]. Additionally, Arora found that a tool shoulder diameter 3x material thickness had ideal sliding and sticking torque properties resulting in higher UTS and reduced thermal input when compared to tool shoulders with smaller and larger diameters respectively [31]. For these reasons, a tool shoulder with a diameter of 19 mm was used for welding the material thickness of 6.35 mm. A tool shoulder with a diameter of 25.4 mm, which was four times material thickness, was also assessed to compare UTS and ductility due to grain elongation from additional heat input from a larger shoulder diameter. A study on AA2014 found that added heat input from a larger tool shoulder may also cause surface defects due to excessive plastic deformation at the shoulder-material interface [32]. Tensile tests were performed on the sample welds using a Zwick/Roell 100 kN ProLine tensile test stand with a Zwick/Roell Type 8406 50 kN load cell, as shown in Fig 3. The ProLine machine has a drive system positional repeatability of  $\pm 2 \mu\text{m}$  and a data transfer rate of 500 Hz [33]. Test coupons were cut to the size of 80 mm x 12.7 mm x 4 mm. Sample dimensions in mm are shown in Fig 4. To ensure sample uniformity, after welding, the top surface was machined to remove flash and create a smooth surface free of defects. The underside was then machined to a final thickness of 4 mm for consistent sample dimensions.

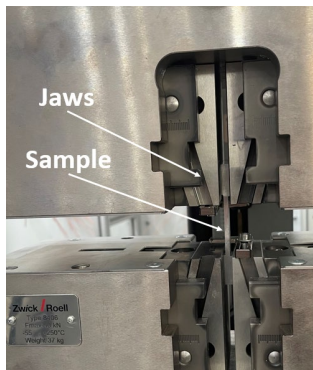


Figure 3 – Sample in tensile machine.

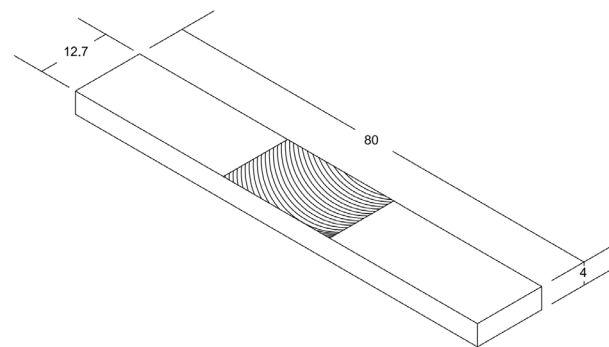


Figure 4 – Tensile sample (dim. in mm).

The parameter set for this study is shown in Table 2. For each set there were two samples cut for testing. Feed rates ranging from 100 mm/min up to 700 mm/min were evaluated along with varying tool shoulder diameters and tool rotation speeds. It is worth noting that this study was initiated as a response to an industry need for achieving the highest possible UTS from FSW AA3003-H14 completed in a 5-axis CNC.

*Table 2 – Test Parameters.*

Set # Parameter	1	2	3	4	5	6	7	8	9	10	11
Shoulder Diameter (mm)	25.4			19							
Tool Rotation Speed (rpm)	1200			1200			1400				
Feed Rate (mm/min)	100	200	300	300	400	500	300	400	500	600	700

Therefore, several trials with varying parameters took place to achieve the required goal and hence some parameter combinations were not examined. Having a full-factorial parameter was not initially intended. Ergo, some combinations are missing in the work presented herein. However, this study presents the obtained results before testing was terminated. The top surface of welded samples prepared for tensile testing are shown in Fig. 5. All samples were evaluated at room temperature in a thermally stable facility. The weld seam centerline is shown as a black dotted line across the samples. Note that samples 1-3 are pictured before machining was performed.

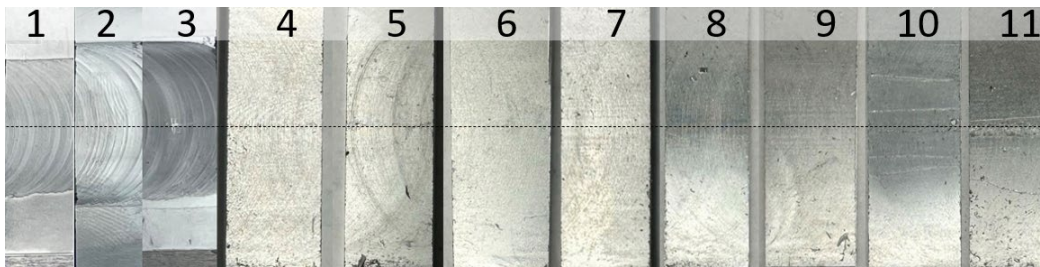


*Figure 5 – Top view of samples prepared for testing. Black dotted line represents center of weld seam.*

## Results

A base metal (BM) sample was tested as a baseline and exhibited a UTS of 155 MPa which is nominal for this material. To evaluate the influence of grain orientation on the weld sample tensile test results, an isotropic tensile test was performed on eighteen BM samples. Samples were laser cut from the BM in orientations of 0°, 45° and 90°. Laser cuts were performed on a Trumpf TruFlow 4000W CO<sub>2</sub> laser. Tensile tests were performed to identify the influence grain orientation had on the UTS of the welded samples. For each orientation there were six samples cut for a population size of eighteen samples. UTS results of the samples in each orientation are below in Table 3. It can be seen that average tensile variation within each orientation group was <1 MPa. It can also be seen there was a pooled standard deviation of 0.624 for the entire population. The variation in UTS for each orientation of the base metal did not play a significant role in affecting tensile strength of the welded samples.

The results for welded sample tensile tests are shown in Fig. 6. Various weld parameters were assessed in eleven different sets of welds. The welding parameters with the best results from this study produced a UTS of 94% base metal strength utilizing a 25.4 mm shoulder, feed rate of 100 mm/min and tool rotation speed of 1200 rpm. A decline in UTS was found when the tool shoulder diameter was reduced from 25.4 mm to 19 mm. Altering feed rates showed a slight change in strength while tool rotational speed did not have a significant effect on UTS in this study. Destruct samples from each set are displayed in Fig. 7. Fractures mainly occurred outside of the weld zone while samples 1-3 and 11 fractured within the weld zone. Ductile fractures outside the weld zone showed signs of necking while fractures in the weld zone exhibit stronger less ductile breakages. These results coincide with studies conducted by Goa on thin sheets of FSW AA3003 [34].

Table 3 – BM UTS results

Orientation	UTS (MPa)	AVG UTS (MPa)	Std. Dev	95% CI
0°	161	162 ± 0.5	0.753	(161.291, 162.376)
	163			
	162			
	162			
	162			
	161			
45°	157	157 ± 0.5	0.548	(155.957, 157.043)
	156			
	157			
	156			
	157			
	156			
90°	163	163 ± 0.5	0.548	161.957, 163.043)
	162			
	162			
	163			
	162			
	163			
		Pooled Std. Dev	0.624	

The average delta length at break ( $L_{b\Delta}$ ) for the BM samples was  $5.88 \text{ mm} \pm 1.5 \text{ mm}$  with a minimum  $L_{b\Delta}$  of 4.4 mm. The  $L_{b\Delta}$  for the most optimal weld parameter sample in this study was 4 mm which is 90% the  $L_{b\Delta}$  of the minimum BM sample. This coincides with an article where Boopathi notes optimal weld parameters can yield ductility in the weld nugget matching, sometimes exceeding, BM ductility in tensile tests [35]. Hardness testing across the weld zone, shown in Fig. 8, was done on Sample 1, welded at 100 mm/min, and Sample 2, welded at 200 mm/min. The stir zone (SZ) in Sample 2 exhibited higher hardness than the Thermomechanically affected zone (TMAZ). Inversely, the SZ in Sample 1 had a lower hardness than both the TMAZ and HAZ even though this sample had a higher UTS than Sample 2. This may be attributed to higher heat input causing more plastic deformation which creates a softer SZ, relative to the other sample [24].

**Conclusion**

The parametric variable with the largest effect on joint strength was the diameter of the tool shoulder while feed rate played a lesser role. A 17.7% reduction in UTS was found when shoulder diameter was reduced from 25.4 mm to 19 mm. This was the largest variation among the parameters in the data set. An increased feed rate with a larger shoulder diameter decreased UTS, while an increased feed rate with a smaller shoulder diameter had mixed effects on UTS. This may be attributed to multiple factors affecting the heat generation and level of mixing within the weld.

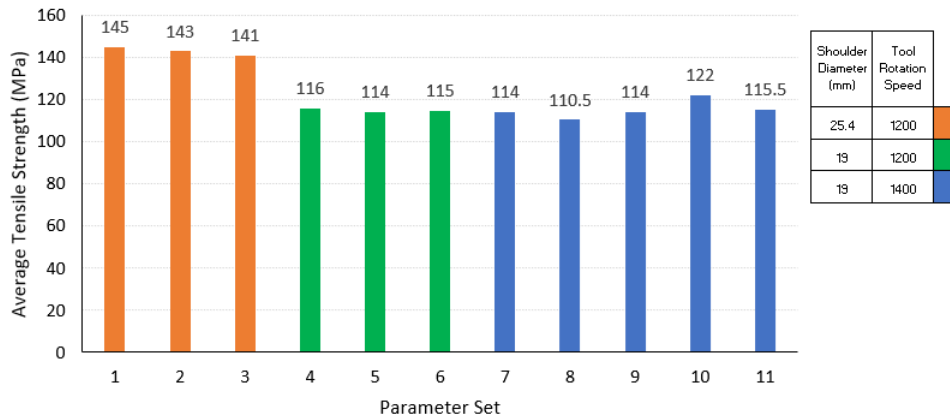


Figure 6 – Average UTS in MPa.

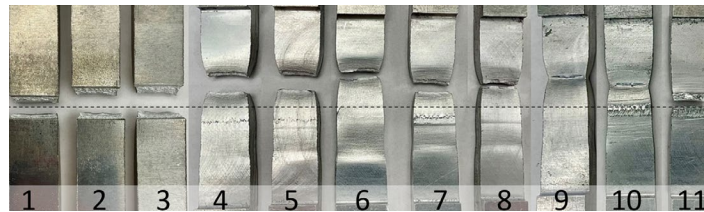


Figure 7 – Destruct samples with weld seam shown as black dotted line.

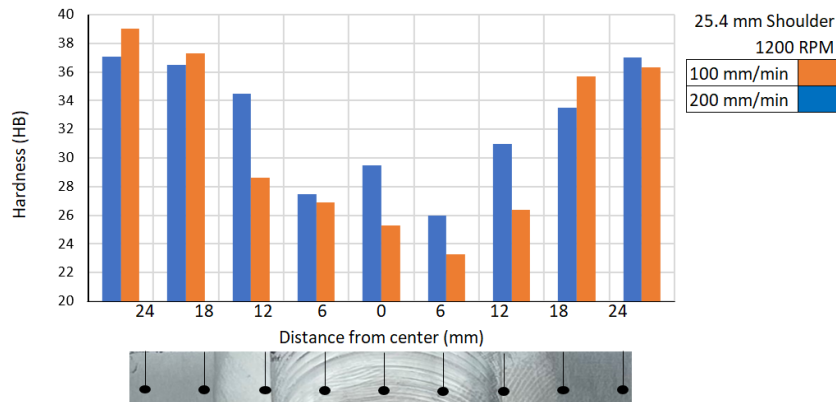


Figure 8 – Brinell Hardness across material zones.

Tool rotation speed did not exhibit a significant effect on weld strength in this study; however, there was notably a minor difference of just 200 rpm between sets comparatively. These results agree with previous research noted in the literature [18]. However, the results related to shoulder diameter do not agree with some findings in the literature [31]. This may be attributed to the differences between AA6061, which is reported in literature, and AA3003 reported in this study. AA6061 is a heat treatable alloy, while AA 3003 is non-heat treatable, which may play a role in the contrasting results. Additionally, the larger shoulder diameter may have created more heat input which has been shown to result in a more homogeneous and defect-free weld as opposed to welds with less heat input [36]. As previously noted, excess thermal input from increased shoulder diameters may negatively affect the surface appearance from excessive plastic deformation but does not affect the quality of the weld [32]. These results provide a valuable analysis on parametric effects on joint strength of friction stir welded AA3003 in a horizontal 5-axis CNC. Based on the experimental results and observations, the following conclusions are drawn:

- A shoulder diameter of four times material thickness produced higher joint strength (94% that of base metal) than welds performed with a shoulder diameter three times material thickness (79% that of base metal).
- Increasing feed rate with a 19 mm shoulder had varied effects on joint strength while increasing feed rate with a 25.4 mm shoulder had unfavourable effects (a decrease of 2.8%).
- Varying tool rotation speed in this study did not have a significant impact on joint strength. A 16% increase in tool rotation speed, from 1200 to 1400 rpm, resulted in a 1% increase in UTS. This increase of 200 rpm may not have been a large enough change in tool rotation speed to cause a noticeable effect.

### Acknowledgement

The author would like to thank colleagues from GROB Systems Inc. and GROB-WERKE GmbH & Co. KG for their support in completing the welding and mechanical testing of this research study.

### References

- [1] Dixit, P., & Dixit, U. (2008). *Modeling of Metal Forming and Machining Processes*. Springer London. <https://doi.org/10.1007/978-1-84800-189-3>
- [2] Vignesh, R. V., Padmanaban, R., & Govindaraju, M. (Eds.). (2023). *Advances in Processing of Lightweight Metal Alloys and Composites: Microstructural Characterization and Property Correlation*. Springer Nature Singapore. <https://doi.org/10.1007/978-981-19-7146-4>
- [3] Singh, B. R. (2012). *A Hand Book on Friction Stir Welding*. LAP Lambert Academic Publishing, UK. <https://doi.org/10.13140/RG.2.1.5088.6244>
- [4] Kumar, A., Gautam, S. S., & Kumar, A. (2014). Heat Input & Joint Efficiency of Three Welding Processes TIG, MIG and FSW using AA606. *International Journal of Mechanical Engineering and Robotics Research*, 91-92.
- [5] Takhakh, A. M., & Abdullah, A. M. (2011). An Experimental Investigation on Fatigue Properties of AA3003-H14 Aluminum alloy Friction Stir Welds. *Journal of Engineering*, 17(06), 1391–1401. <https://doi.org/10.31026/j.eng.2011.06.07>
- [6] Mypati, O., Mishra, D., Sahu, S., Pal, S. K., & Srirangam, P. (2020). A Study on Electrical and Electrochemical Characteristics of Friction Stir Welded Lithium-Ion Battery Tabs for Electric Vehicles. *Journal of Electronic Materials*, 49(1), 72–87. <https://doi.org/10.1007/s11664-019-07711-8>
- [7] European Aluminum Association. (2011). *The Aluminum Automotive Manual*.
- [8] Dellal, N., Merzoug, M., Mimmi, A., Ghazi, A., & Lousdad, A. (2023). Experimental based determination and analysis of mechanical properties of AA 3003 alloy welded with friction stir lap welding process. *Journal of Applied Engineering Science*, 21(2), 451–461. <https://doi.org/10.5937/jaes0-40245>.
- [9] Kelly, J. F., & Cotterell, M. G. (2002). Minimal lubrication machining of aluminium alloys. *Journal of Materials Processing Technology*, 120(1–3), 327–334. [https://doi.org/10.1016/S0924-0136\(01\)01126-8](https://doi.org/10.1016/S0924-0136(01)01126-8).
- [10] Santos, M. C., Machado, A. R., Sales, W. F., Barrozo, M. A. S., & Ezugwu, E. O. (2016). Machining of aluminum alloys: A review. *The International Journal of Advanced Manufacturing Technology*, 86(9–12), 3067–3080. <https://doi.org/10.1007/s00170-016-8431-9>.

- [11] Mendes, N., Neto, P., Loureiro, A., & Moreira, A. P. (2016). Machines and control systems for friction stir welding: A review. *Materials & Design*, 90, 256–265. <https://doi.org/10.1016/j.matdes.2015.10.124>
- [12] Ižol, P., Varga, J., Vrabel, M., Demko, M., Greš, M., (2022). Evaluation of 3-Axis and 5-Axis Milling Strategies when Machining Freeform Surface Features. Technical University of Košice, Faculty of Mechanical Engineering, Prototyping and Innovation Centre, Košice, Slovakia. *Journal of Production Engineering*, 25(1), 1–4. <https://doi.org/10.24867/JPE-2022-01-001>.
- [13] Bologa, O., Breaz, R.-E., Racz, S.-G., & Crenganiș, M. (2016). Decision-making Tool for Moving from 3-axes to 5-axes CNC Machine-tool. *Procedia Computer Science*, 91, 184–192. <https://doi.org/10.1016/j.procs.2016.07.056>
- [14] Meyghani, B., & Awang, M. (2022). The Influence of the Tool Tilt Angle on the Heat Generation and the Material Behavior in Friction Stir Welding (FSW). *Metals*, 12(11), 1837. <https://doi.org/10.3390/met12111837>.
- [15] Davim, J. P. (Ed.). (2015). *Modern Manufacturing Engineering*. Springer International Publishing. <https://doi.org/10.1007/978-3-319-20152-8>.
- [16] Wang, X., Xiao, Y., Shi, L., Zhai, M., Wu, C., & Chen, G. (2023). Revealing the mechanism of tool tilting on suppressing the formation of void defects in friction stir welding. *Journal of Materials Research and Technology*, 25, 38–54. <https://doi.org/10.1016/j.jmrt.2023.05.184>
- [17] Thomas, W. M., Braithwaite, A. B. M., & John, R. (2001, September 27). SKEW-STIR™ TECHNOLOGY. 3rd International Symposium on Friction Stir, Kobe, Japan.
- [18] Goyal, A., Punit Kumar Rohilla, & Atul Kumar Kaushik. (2017). Optimization of Friction Stir Welding Parameters for AA3003 Aluminum Alloy Joints Using Response Surface Methodology. *Atul Kumar Kaushik*, 12(1), 15–26. <http://www.ripublication.com/ijms.htm>
- [19] Meyghani, B., Awang, M., & Wu, C. S. (2020). Finite element modeling of friction stir welding (FSW) on a complex curved plate. *Journal of Advanced Joining Processes*, 1, 100007. <https://doi.org/10.1016/j.jajp.2020.100007>
- [20] Xiao, X., Mao, Y., Wang, X., Qin, D., & Fu, L. (2023). Effects of Curvature Direction on Friction Stir Welding Lap Joint of Aluminum Alloy “S” Curved Surface. In Review. <https://doi.org/10.21203/rs.3.rs-2432943/v1>
- [21] Longhurst, W. R., Strauss, A. M., Cook, G. E., & Fleming, P. A. (2010). Torque control of friction stir welding for manufacturing and automation. *The International Journal of Advanced Manufacturing Technology*, 51(9–12), 905–913. <https://doi.org/10.1007/s00170-010-2678-3>.
- [22] Chandu, K, Rao, A, & Subrahmanyam, B. (2014). The Strength of Friction Stir Welded Aluminum Alloy 6061. *International Journal of Research in Mechanical Engineering & Technology*, 119.
- [23] Xu, A. (2020). Properties of Friction Stir Welded 3003-H17 Aluminum Alloy at High Travel Speeds. *Journal of Physics: Conference Series*, 1676(1), 012114. <https://doi.org/10.1088/1742-6596/1676/1/012114>
- [24] Takhakh, D. A. M., & Abdullah, A. M. (2012). The Optimization Conditions of Friction Stir Welding (FSW) for Different Rotational and Weld speeds. *Nahrain University, College of Engineering Journal*, 15(2), 187–196.

- [25] Kasman, Ş. (2022). Characterization of friction stir welded AA 3003-H24 aluminum alloy plates. *Sigma Journal of Engineering and Natural Sciences – Sigma Mühendislik ve Fen Bilimleri Dergisi*. <https://doi.org/10.14744/sigma.2022.00066>
- [26] Shalin, M., & Hiten, M. (2018). Experimental Analysis on Effect of Tool Transverse Feed, Tool Rotational Speed and Tool Pin Profile Type on Weld Tensile Strength of Friction Stir Welded Joint of AA 6061. *Materials Today: Proceedings*, 5(1), 487–493. <https://doi.org/10.1016/j.matpr.2017.11.109>
- [27] MatWeb. (2024). *Aluminum 3003-H14*. Retrieved from <https://www.matweb.com/search/DataSheet.aspx?MatGUID=09c63ea8e10e4eea8398256801bb8514>
- [28] GROB-WERKE. (2023). *G550T 5-axis universal mill-turn machining center*. Retrieved from Grob: <https://www.grobgroup.com/en/products/product-range/universal-machining-centers/mill-turn-machining-centers/g550t/>
- [29] Padmanaban, G., & Balasubramanian, V. (2009). Selection of FSW tool pin profile, shoulder diameter and material for joining AZ31B magnesium alloy – An experimental approach. *Materials & Design*, 30(7), 2647–2656. <https://doi.org/10.1016/j.matdes.2008.10.021>
- [30] Elangovan, K., & Balasubramanian, V. (2008). Influences of tool pin profile and tool shoulder diameter on the formation of friction stir processing zone in AA6061 aluminium alloy. *Materials & Design*, 29(2), 362–373. <https://doi.org/10.1016/j.matdes.2007.01.030>
- [31] Arora, A., De, A., & DebRoy, T. (2011). Toward optimum friction stir welding tool shoulder diameter. *Scripta Materialia*, 64(1), 9–12. <https://doi.org/10.1016/j.scriptamat.2010.08.052>
- [32] Ramanjaneyulu, K., Madhusudhan Reddy, G., & Venugopal Rao, A. (2014). Role of Tool Shoulder Diameter in Friction Stir Welding: An Analysis of the Temperature and Plastic Deformation of AA 2014 Aluminium Alloy. *Transactions of the Indian Institute of Metals*, 67(5), 769–780. <https://doi.org/10.1007/s12666-014-0401-z>
- [33] Zwick Roell. (2024). *Materials Testing Machines ProLine Z005 to Z100*. Retrieved from [https://www.zwickroell.com/fileadmin/content/Files/SharePoint/user\\_upload/PI\\_EN/02\\_375\\_ProLine\\_Z005\\_up\\_to\\_Z100\\_Materials\\_Testing\\_Machine\\_PI\\_EN.pdf](https://www.zwickroell.com/fileadmin/content/Files/SharePoint/user_upload/PI_EN/02_375_ProLine_Z005_up_to_Z100_Materials_Testing_Machine_PI_EN.pdf)
- [34] Gao, K., Basak, S., Mondal, M., Zhang, S., Hong, S.-T., Boakye, S. Y., & Cho, H.-H. (2022). Friction stir welding of AA3003-clad AA6013 thin sheets: Microstructural changes related to tensile properties and fatigue failure mechanism. *Journal of Materials Research and Technology*, 17, 3221–3233. <https://doi.org/10.1016/j.jmrt.2022.02.073>
- [35] Boopathi, S. (2017). Review on Effect of Process Parameters—Friction Stir Welding Process. 04(07).
- [36] Abnar, B., Gashtiazar, S., & Javidani, M. (2023). Friction Stir Welding of Non-Heat Treatable Al Alloys: Challenges and Improvements Opportunities. *Crystals*, 13(4), 576. <https://doi.org/10.3390/cryst13040576>